J. Phys. B: At. Mol. Opt. Phys. **32** (1999) 5805–5823. Printed in the UK PII: S0953-4075(99)06843-1

Breit–Pauli energy levels, lifetimes, and transition data: beryllium-like spectra

Georgio Tachiev and C Froese Fischer
Department of Computer Science, Vanderbilt University, Box 1679B, Nashville, TN 37235, USA

Received 11 August 1999, in final form 22 October 1999

Abstract. Breit–Pauli results for energy levels, lifetimes, and some transition data are reported for all levels of the $2s^2$, 2s2p, $2p^2$, 2s3s, 2s3p, and 2s3d configurations of the Be-like spectrum for $4 \leqslant Z \leqslant 12$. A simultaneous optimization scheme was applied so that a radial basis could be determined for a set of terms that mix in the Breit–Pauli approximation. Convergence of the LS line strength is used as a factor in estimating accuracy as well as the agreement of energy levels and their splitting between theory and experiment. The results are evaluated by comparison with other theoretical results and experiment for transition rates.

1. Introduction

Atomic spectroscopic data are essential to many astrophysical studies. Seaton [1], in describing atomic data needed for the calculation of radiative accelerations and diffusion in Mn and HgMn stars, mentioned a need for some 5×10^6 f-values. The Opacity Project [2] was undertaken to produce these huge amounts of data in the LS approximation using close-coupling theory and the R-matrix method. But even in light atoms, the mixing of terms can be important as in the $2p3p\,^3P^o_J$–$2p3d\,^3P^o_J$ transitions which are the primary decays of the Bowen fluorescence mechanism in O III [3]. At the same time, intercombination transitions are of great interest in the study of astrophysical plasmas where they may play an important diagnostic role. The transition rates of such transitions originate entirely from the mixing of terms through spin–orbit and other relativistic effects.

In the last decade, tremendous progress has been realized in variational methods for *ab initio* calculation of atomic properties [4], including also transition rates [5]. Relativistic effects can be included either in a full multiconfiguration Dirac–Fock (MCDF) calculation or through a non-relativistic multiconfiguration Hartree–Fock (MCHF) calculation followed by a configuration interaction calculation using the Breit–Pauli (BP) Hamiltonian. In the former, relativistic effects are incorporated fully into the theory but, because of the resulting complexity, the inclusion of correlation is often limited, particularly in complex systems. The opposite is true of the MCHF + BP approach: more correlation can be included but the relativistic effects are treated only to lowest order. These two approaches have been compared extensively for the $2s^2\,^1S_0$–$2s2p\,^3P^o_1$ transition in C III [6, 7] and with the most accurate experimental A-value [8]. Though both theories are in excellent agreement with experiment, MCHF + BP was computationally much simpler and observed data could be used to improve the mixing of terms.

Recently, BP energies and transition rates were reported for the 2s, 2p, 3s, 3p, 3d, and $3s\,^2L$ terms of the Li-like sequence, $3 \leqslant Z \leqslant 8$ [9]. For neutral Li, the uncertainty in the

transition rates was less than the error of the most accurate experiment. No term mixing was included. In this paper we extend the BP 'spectrum' calculations, where all transitions between levels of a portion of the energy spectrum are computed, to the Be-like states. In anticipation of more complex cases, like in the F-like sequence where the mixing may include as many as six terms, a method of simultaneous optimization was developed and is evaluated here for these simpler, four-electron systems.

2. Computational procedures

The non-relativistic MCHF approach is used for calculating the wavefunction Ψ of the state labelled γLS

$$\Psi(\gamma LS) = \sum_j c_j \Phi(\gamma_j LS), \tag{1}$$

where γ represents the dominant configuration, and any additional quantum numbers required for uniquely specifying the state are considered. The MCHF wavefunction Ψ is expanded in terms of configuration state functions (CSFs) $\{\Phi\}$ having the same LS symmetry but arising from different electronic configurations (γ_j). The CSFs are built from a basis of one-electron spin-orbital functions

$$\phi_{nlm_lm_s} = \tfrac{1}{r} P_{nl}(r) Y_{lm_l}(\theta, \varphi) \chi_{m_s}. \tag{2}$$

The MCHF procedure [10] consists of optimizing to self-consistency *both* the sets of radial functions $\{P_{n_jl_j}(r)\}$ and mixing coefficients $\{c_j\}$. Thus the CSFs included in the expansion determine the radial functions.

In large-scale methods, systematic calculations are performed of increasing size that allow the monitoring of properties under investigation. In such systematic methods, active sets (ASs) of orbitals are used to determine the expansion. These are characterized by the largest principal quantum number. Thus the $n = 3$ AS consists of all the orbitals {1s, 2s, 2p, 3s, 3p, 3d}, though it should be remembered that for correlation orbitals (orbitals not occupied in the Hartree–Fock approximation), the principal quantum number is not important spectroscopically, but serves as a simple index for the orbital of a given symmetry.

Given an active orbital set, rules are used to generate the CSF expansion. In neutral Be, term mixing is negligible but, at the same time, correlation in the core (which modifies the potential for the outer electrons) is more important. For this reason, the rules for generating expansions for states in Be were different from those of the ions.

The rules for obtaining expansions are often expressed in terms of a number of excitations—singles (S), doubles (D), etc. However, in order to allow for the near-degeneracy of the 2s and 2p orbitals at higher Z, it is convenient to express the rule in terms of the set of possible principal quantum numbers. To curb the rate of growth of the expansions with the orbital set size, it may be convenient to define the CSFs set as the union of sets. In this paper, the sets used were the following:

atom: $\{1, 2\}\{1, 2, 3\}\{2, 3, \ldots, n \leqslant 5\}^2 \cup 1\mathrm{s}\{1, 2, 3\}\{2, 3, \ldots, n \leqslant 8\}^2 \cup 1\mathrm{s}^2\{2, 3, \ldots, n\}^2$

ion: $1\mathrm{s}\{1, 2, 3\}\{2, 3, \ldots, n \leqslant 9\}^2 \cup 1\mathrm{s}^2\{2, 3, 4, \ldots, n\}^2$.

In other words, in the first set for the atom, the first electron has a principal quantum number of $n = 1$ or $n = 2$; the second has a principal quantum number in the range $n = 1, 2, 3$, and the last two electrons are unrestricted, but with $n \leqslant 5$. Notice that this rule allows double excitations from $1\mathrm{s}^2$ and hence includes core correlation. The CSFs with one 1s orbital represent core polarization, and those with $1\mathrm{s}^2$ are part of valence correlation. For the ions, core correlation

was neglected so that the computational size could be constrained. In all cases for $n \geqslant 4$, the 1s orbital was fixed being obtained from an expansion over the set $1s^2\{2, 3\}^2$ and all orbitals were varied. Also, all expansions were restricted to $l \leqslant 6$ or i-orbitals.

Once a set of radial orbitals has been obtained, the relativistic corrections can be taken into account within the BP approximation by diagonalizing the BP Hamiltonian [10] to get the intermediate coupling wavefunctions

$$\Psi(\gamma J) = \sum_{LS} \sum_{j} c_j(LS)\Phi(\gamma_j LSJ). \tag{3}$$

Thus the expansion is now the sum of expansions over a set of terms. For all expansions, the iterative Davidson method [11] was used to determine a few of the lowest eigenvalues and eigenvectors [12].

All the results in this paper, unless specifically stated as being LS results, are based on the diagonalization of the BP Hamiltonian in which the orbit–orbit term has been omitted. This operator does not contribute to the mixing of terms, and behaves like a small correlation correction. Experiments in Li-like spectra [9] have shown that inclusion of orbit–orbit can double the computation times for generating the BP interaction matrix, yet have negligible effect at the present level of accuracy. For this reason, it has been omitted, as is common practice. In the rest of the paper, we will refer to our results as MCHF results, and only use MCHF + BP for emphasis, when needed.

The weighted oscillator strengths gf are calculated using the length and velocity formalisms

$$g_i f_l(\mathrm{i}k) = \tfrac{2}{3}\Delta E_{ik}|\langle\Psi_i\|\sum_j \mathbf{r}_j\|\Psi_k\rangle|^2 \tag{4}$$

$$g_i f_v(\mathrm{i}k) = \frac{2}{3}\frac{1}{\Delta E_{ij}}|\langle\Psi_i\|\sum_j \boldsymbol{\nabla}_j\|\Psi_k\rangle|^2 \tag{5}$$

to monitor the expected convergence between the two forms with the improvement of the wavefunction Ψ_i of the lower state and Ψ_k of the upper state, and of the corresponding transition energy ΔE_{ik}. In these equations, g_i is the degeneracy factor, i.e. $g_i = (2L_i + 1)(2S_i + 1)$ for LS-coupled wavefunctions and $g_i = (2J_i + 1)$ for BP wavefunctions. In the BP approximation, the above length form is correct to $O(\alpha^2)$ (except for the omission of orbit–orbit) while the velocity form requires a relativistic correction to the gradient operator [13]. For this reason, it is customary to report both length and velocity results for an LS calculation, but only the length form in the BP calculation.

No orthonormality constraints are imposed *between* the two sets of radial functions spanning the two total wavefunctions Ψ_i and Ψ_k, allowing a *separate* MCHF optimization of the two states involved. The details of the bi-orthonormal transformation algorithm used for dealing with the resulting non-orthogonality problems can be found elsewhere [14].

3. Optimization strategies

The usual MCHF variational optimization method for a given term, produces term-dependent orbitals. The BP code, however, requires that the orbitals for each term be the same. When only two terms are mixed, the $(n, n + 1)$ scheme [10] works well where orbitals are optimized systematically for a primary term and then an extra 'layer' of orbitals is optimized on the secondary term. When many terms are present, this scheme becomes unmanageable if extended to an $(n, n + 1, \ldots, n + m - 1)$ procedure for the mixing of m terms. Simplifying assumptions could be made using a cross-optimization scheme [15], but these tend to be somewhat arbitrary.

Table 1. Optimization strategies for groups of terms and their J values.

States	Terms
$2s^2\,{}^1S_0$	$2s^2\,{}^1S$, $2p^2\,{}^3P$
$2p^2\,{}^3P_{0,1,2}$, ${}^1D_2$, ${}^1S_0$	$2p^2\,{}^3P$, ${}^1D$, ${}^1S$
$2s3s\,{}^1S_0$, ${}^3S_1$	$2s3s\,{}^1S$, ${}^3S$ and $2p^2\,{}^3P$
$2s3d\,{}^1D_2$, ${}^3D_{1,2,3}$	$2s3d\,{}^1D$, ${}^3D$ and $2p^2\,{}^1D$, ${}^3P$
$2s2p\,{}^1P^o_1$, ${}^3P^o_{0,1,2}$	$2s2p\,{}^1P^o$, ${}^3P^o$
$2s3p\,{}^1P^o_1$, ${}^3P^o_{0,1,2}$	$2s3p\,{}^1P^o$, ${}^3P^o$

The MCHF optimization is based on an energy functional for a given LS term. In this work, we have extended the code to simultaneous optimization of a weighted average of energy functionals of one or more terms, where the weights can be user defined. At the same time, it is also possible to optimize on one or more eigenvalues of a given term, again with user defined weights, though the weights for all the eigenvalues of a specific term were assumed to be the same. Suppose $\mathcal{E}(T_i)$ represents an energy functional for term T and eigenvalue i, assuming orbitals and also wavefunctions are normalized. Then optimization was performed on the functional

$$\mathcal{E} = \sum_{T_i} w_{T_i} \mathcal{E}(T_i) / \sum_{T_i} w_{T_i}$$

where w_{T_i} is the weight for T_i.

The different states of the Be-like ions were grouped together and a radial basis determined for a set of terms and/or eigenvalues that were deemed to be important for the relativistic effects, as shown in table 1. All had equal weights. Thus 2d 3d ${}^1D_2$, ${}^3D_{1,2,3}$ states were computed from a mixing of three terms: ${}^1D$, ${}^3D$ and ${}^3P$, but two lowest eigenvalues from the ${}^1D$ expansion were included in the expression of the energy functional for optimization of orbitals, along with the lowest from ${}^3D$, and the lowest from ${}^3P$. A question arises as to how the 1s orbitals are to be determined. Since the mixing of $2p^2\,{}^3P_0$ with $2s^2\,{}^1S_0$ is rather small, even for our highest Z, it was found that a better spectrum was obtained if the 1s orbital was obtained from an $n = 3$ expansion over ${}^1S$ only. In all other cases, the 1s orbital was determined from simultaneous optimization at the $n = 3$ level of all the terms as indicated in table 1. After that, for expansions with $n \leqslant 5$, all orbitals except 1s were varied; for $n = 6$, all but 1s, 2s, 2p were varied and, in the case of 2s3p and 2s3d, all but 1s, 2s, 2p, 3s, 3p, 3d. For $n = 7$ and $n = 8$, the last 20 orbitals were varied except for the $n = 7$ calculations for 2s3p and 2s3d where the number was 18. For $n = 9, 10$, only the new orbitals were varied, all others being kept fixed.

The neutral atom was treated somewhat differently. As already mentioned, core correlation is more important here and was included in the model. At the same time, the only term mixing included in the calculations was the singlet-triplet mixing of 2s2p and 2s3p.

4. Evaluation of the simultaneous optimization process

In a non-relativistic, independent optimization process, convergence of the transition energy and the agreement of the length and velocity forms of the line strength can be used as indicators of accuracy. The transition energies themselves may differ from observed transition energies because of omitted correlation and relativistic effects. In table 2, the non-relativistic transition energies and line strengths (length and velocity form) for simultaneous and independent optimization are compared for transitions in B II. This table shows that, for expansions up to $n = 10$, the orbital bases from the two methods yield results which generally differ by less

Table 2. Convergence of the LS line strength S for simultaneous and independent optimization in B II. S_l is the length form and S_v the velocity form. The notation E + $(-)n$ denotes $\times 10^n$. The results from simultaneous optimization appear above those for independent optimization. The difference (in %) is relative to the average of S_l and S_v.

Transition	E (cm^{-1})	S_l	S_v	Difference (%)
$2s^2\,{}^1S$–$2s2p\,{}^1P^o$	73 445.70	4.479 4E+00	4.483 7E+00	0.095 9
	73 447.14	4.479 3E+00	4.484 1E+00	0.107 1
$2s^2\,{}^1S$–$2s3p\,{}^1P^o$	144 145.15	2.485 0E−01	2.485 2E−01	−0.007 2
	144 146.56	2.486 0E−01	2.486 1E−01	−0.004 8
$2s2p\,{}^3P^o$–$2s3d\,{}^3D$	113 349.86	1.244 6E+01	1.241 6E+01	0.241 3
	113 349.83	1.242 3E+01	1.241 6E+01	0.056 4
$2s2p\,{}^3P^o$–$2p^2\,{}^3P$	61 711.52	1.645 5E+01	1.640 2E+01	0.322 6
	61 706.14	1.645 6E+01	1.640 3E+01	0.322 6
$2s2p\,{}^3P^o$–$2s3s\,{}^3S$	92 428.25	2.052 1E+00	2.037 4E+00	0.718 9
	92 427.81	2.046 2E+00	2.038 4E+00	0.381 9
$2s2p\,{}^1P^o$–$2p^2\,{}^1D$	29 076.81	5.505 1E+00	5.449 3E+00	1.018 8
	29 076.70	5.504 7E+00	5.448 3E+00	1.029 9
$2s2p\,{}^1P^o$–$2s3d\,{}^1D$	81 303.55	6.267 6E+00	6.284 9E+00	−0.275 6
	81 303.57	6.266 3E+00	6.284 8E+00	−0.294 8
$2s2p\,{}^1P^o$–$2p^2\,{}^1S$	54 378.01	4.102 5E+00	4.102 3E+00	0.004 9
	54 377.92	4.102 1E+00	4.102 5E+00	−0.009 8
$2s2p\,{}^1P^o$–$2s3s\,{}^1S$	64 260.02	2.651 0E−03	2.225 2E−03	17.464 4
	64 259.69	2.657 6E−03	2.212 2E−03	18.292 3
$2p^2\,{}^3P$–$2s3p\,{}^3P^o$	44 957.20	2.651 8E−03	2.376 9E−03	10.933 2
	44 962.58	2.631 4E−03	2.399 6E−03	9.214 9
$2p^2\,{}^1D$–$2s3p\,{}^1P^o$	41 622.65	1.537 7E+00	1.567 1E+00	−1.893 8
	41 622.71	1.538 5E+00	1.566 7E+00	−1.816 3
$2s3s\,{}^3S$–$2s3p\,{}^3P^o$	14 240.91	6.142 8E+01	6.117 0E+01	0.420 9
	14 240.47	6.143 9E+01	6.119 4E+01	0.399 6
$2p^2\,{}^1S$–$2s3p\,{}^1P^o$	16 321.45	3.993 3E+00	3.977 7E+00	0.391 4
	16 321.49	3.993 9E+00	3.980 9E+00	0.326 0
$2s3s\,{}^1S$–$2s3p\,{}^1P^o$	6 439.44	1.522 7E+01	1.533 2E+01	−0.687 2
	6 439.72	1.522 7E+01	1.533 0E+01	−0.674 1
$2s3p\,{}^1P^o$–$2s3d\,{}^1D$	10 604.09	4.330 6E+01	4.313 1E+01	0.404 9
	10 604.16	4.330 9E+01	4.312 7E+01	0.421 1
$2s3p\,{}^3P^o$–$2s3d\,{}^3D$	6 081.13	1.193 7E+02	1.196 3E+02	−0.217 6
	6 081.11	1.193 3E+02	1.196 9E+02	−0.301 2

than 0.1%. An exception is the length form of the $2s2p\,{}^3P^o$–$2s3d\,{}^3D$ and $2s2p\,{}^3P^o$–$2s3s\,{}^3S$ where trends show the velocity form to be the more stable and so the differences from the two models are somewhat larger, but still less than 0.4%. Others are the two transitions, $2s2p\,{}^1P^o$–$2s3s\,{}^1S$ and $2p^2\,{}^3P$–$2s3p\,{}^3P^o$, where the line strength is exceedingly small. Except when the line strength is small, the difference in length and velocity forms themselves are generally less than 1%, though there is variation.

For the neutral atom, or ions with low degrees of ionization, term dependence can be expected to be larger. Intuitively, independent optimization should produce accurate transition data with a smaller basis. This is shown in figure 1 for $2s2p\,{}^3P^o$–$2p^2\,{}^3P$ and $2s2p\,{}^3P^o$–$2s3d\,{}^3D$ transitions in B II. Here it is seen that independent optimization (lighter lines) converges faster, has the smoother convergence trend, particularly at low n, and that for these two transitions the two optimization schemes converge to about the same length or velocity line strength at $n = 10$. For the former transition, because of the large scale, length and velocity appear not to

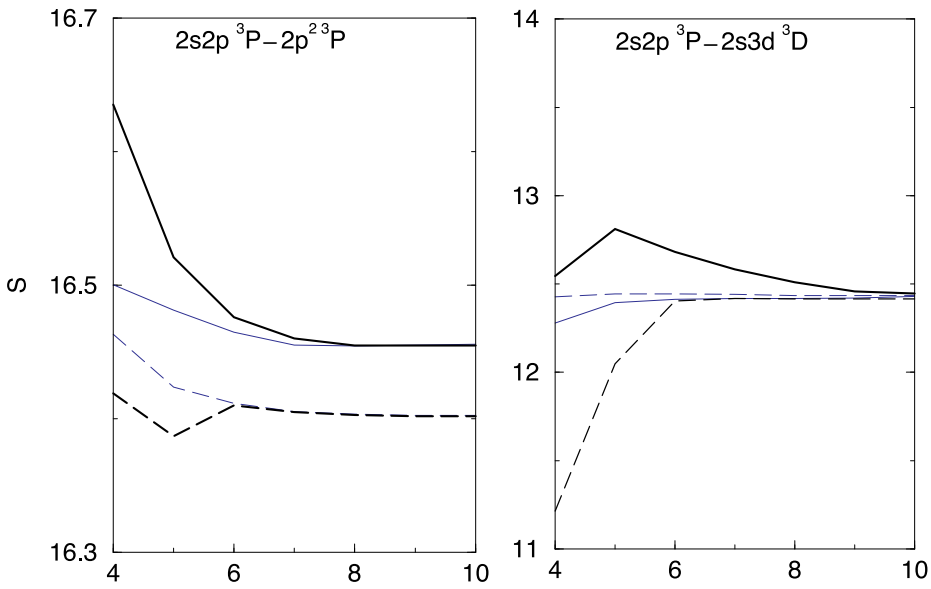

Figure 1. Comparison of convergence of the line strength for independent (light curves) and simultaneous (dark curves) optimization. S_l: solid curves; S_v: dashed curves.

be in good agreement, although, in fact, the difference is only 0.32%. The second transition is somewhat different. The 2s3d ^{1}D has a strong interaction with 2p^2 ^{1}D. At the Hartree–Fock level the latter lies above the 2s4d ^{1}D [16] and a few layers of correlation orbitals are needed to obtain the correct spectrum. Similar problems do not exist for the 2s3d ^{3}D state and independent optimization converges rapidly. When optimizing simultaneously, the ^{3}D state can be expected to have a different convergence pattern since the orbitals now also need to represent the 2s3d ^{1}D state. It is interesting to note that the velocity form for the two optimization schemes converges more rapidly than the length form. This probably is related to the emphasis on the inner region for the velocity form: independent and simultaneous optimization can be expected to differ more in the outer regions. For many transitions, like 2s2p ^{3}P^o–2p^2 ^{3}P, the LS trends have converged already at $n = 8$, but for others such as 2s2p ^{3}P^o–2s3d ^{3}D or 2s2p ^{1}P^o–2s3s ^{1}S^o, where the line strength is extremely small due to cancellation (see table 2) the larger basis was needed.

5. Breit–Pauli results

The orbital basis from simultaneous optimization may be used to determine J-dependent energy levels and transition rates. In table 3 we report the lifetimes of all the levels of the configurations considered in this work. These are based primarily on the allowed E1 transitions between the different states but the M2 transitions, 2s^2 ^{1}S$_0$–2s2p ^{3}P$^o_2$, were also computed as well as the E2 and M1 transitions, 2s2p ^{3}P$^o_{0,1}$–2s2p ^{3}P$^o_2$, which contribute to the lifetime of the latter. In other cases, the contributions from these forbidden transitions to the lifetime are negligible but calculations were also performed for 2s2p ^{3}P$^o_{0,1,2}$–2s2p ^{1}P$^o_1$. A complete set of transition data (transition energies, line strength, oscillator strengths, transition rates) is available at http://www.vuse.vanderbilt.edu/∼cff/mchf_ collection. This site also reports LS convergence trends, including the length and velocity forms of the line strength, which we will

Table 3. Theoretical lifetimes (in s) for excited states up to $2s3d\,^1D_2$ of Be-like systems for $Z = 4, \ldots, 12$. The notation E + $(-)n$ denotes $\times 10^n$.

Term	J	Z = 4	Z = 5	Z = 6	Z = 7	Z = 8	Z = 9	Z = 10	Z = 11	Z = 12
$2s2p\,^3P^o$										
	1	2.307 0E+00	9.605 8E−02	9.616 0E−03	1.725 6E−03	4.371 5E−04	1.389 9E−04	5.188 7E−05	2.182 8E−05	1.006 6E−05
	2	5.872 6E+03	5.792 1E+02	1.916 2E+02	8.606 1E+01	4.519 8E+01	2.537 7E+01	1.397 2E+01	6.933 8E+00	2.999 0E+00
$2s2p\,^1P^o$	1	1.786 1E−09	8.331 3E−10	5.651 5E−10	4.305 9E−10	3.480 1E−10	2.915 4E−10	2.501 1E−10	2.181 6E−10	1.925 4E−10
$2p^2\,^3P$	0	2.370 3E−09	1.146 3E−09	7.571 4E−10	5.665 9E−10	4.530 0E−10	3.769 9E−10	3.222 1E−10	2.803 2E−10	2.470 7E−10
	1	2.370 2E−09	1.146 1E−09	7.567 5E−10	5.660 1E−10	4.521 8E−10	3.758 9E−10	3.207 7E−10	2.785 1E−10	2.448 3E−10
	2	2.370 0E−09	1.145 7E−09	7.561 6E−10	5.651 1E−10	4.509 0E−10	3.742 1E−10	3.186 6E−10	2.759 8E−10	2.419 3E−10
$2p^2\,^1D$	2	8.185 6E−04	1.817 4E−08	7.191 3E−09	4.266 0E−09	2.967 9E−09	2.243 7E−09	1.781 5E−09	1.456 5E−09	1.212 7E−09
$2p^2\,^1S$	0		7.471 2E−10	4.763 8E−10	3.398 8E−10	2.609 7E−10	2.104 6E−10	1.754 5E−10	1.495 9E−10	1.296 2E−10
$2s3s\,^3S$	1	6.613 3E−09	9.134 1E−10	2.709 2E−10	1.107 6E−10	5.429 0E−11	2.987 2E−11	1.785 5E−11	1.134 8E−11	7.566 5E−12
$2s3s\,^1S$	0	2.988 6E−08	5.956 3E−06	1.170 8E−09	3.826 0E−10	1.753 1E−10	9.418 5E−11	5.587 5E−11	3.546 3E−11	2.367 2E−11
$2s3p\,^1P^o$	1	6.999 6E−08	1.692 5E−09	2.511 8E−10	7.589 3E−11	3.106 0E−11	1.513 9E−11	8.288 1E−12	4.935 8E−12	3.139 8E−12
$2s3p\,^3P^o$	0	8.321 1E−08	2.498 1E−08	1.351 5E−08	8.338 6E−09	5.107 4E−09	3.043 2E−09	1.807 2E−09	1.099 2E−09	6.942 3E−10
	1	8.320 8E−08	2.481 6E−08	1.339 9E−08	8.078 0E−09	4.582 3E−09	2.284 3E−09	9.962 3E−10	3.950 6E−10	1.502 5E−10
	2	8.319 6E−08	2.495 6E−08	1.347 3E−08	8.276 0E−09	5.026 6E−09	2.959 4E−09	1.731 0E−09	1.034 2E−09	6.398 6E−10
$2s3d\,^3D$	1	5.141 2E−09	4.076 9E−10	9.399 8E−11	3.295 2E−11	1.449 8E−11	7.369 9E−12	4.141 5E−12	2.506 0E−12	1.605 1E−12
	2	5.141 2E−09	4.077 2E−10	9.401 5E−11	3.296 4E−11	1.450 6E−11	7.376 1E−12	4.146 4E−12	2.510 2E−12	1.608 6E−12
	3	5.141 4E−09	4.077 8E−10	9.404 4E−11	3.298 2E−11	1.451 8E−11	7.385 7E−12	4.154 1E−12	2.516 4E−12	1.613 9E−12
$2s3d\,^1D$	2	1.248 4E−08	7.214 0E−10	1.588 7E−10	5.399 6E−11	2.326 5E−11	1.164 7E−11	6.471 9E−12	3.880 9E−12	2.467 7E−12

Table 4. Comparison of computed spectrum for O v with tabulated NIST [37] data.

			Level (cm^{-1})			Splitting (cm^{-1})		
Configuration	Term	J	Theory	Observation	Difference	Theory	Observation	Difference
2s2p	$^3P^o$	0	81 985.55	81 942.5	43.05			
		1	82 122.69	82 078.6	44.09	137.14	136.1	1.04
		2	82 429.97	82 385.3	44.67	444.20	442.80	0.58
	$^1P^o$	1	158 933.17	158 797.7	135.47			
$2p^2$	^3P	0	213 794.44	213 462.5	331.94			
		1	213 951.36	213 618.2	333.16	156.92	155.7	1.22
		2	214 220.31	213 887.0	333.31	425.87	424.5	0.15
	^1D	2	232 119.96	231 721.4	398.56			
	^1S	0	288 434.36	287 910.3	524.06			
2s3s	^3S	1	547 153.70	546 972.7	181.00			
	^1S	0	561 500.34	561 276.4	223.94			
2s3p	$^1P^o$	1	581 027.89	580 824.9	202.99			
	$^3P^o$	0	582 986.32	582 806.4	179.92			
		1	583 023.21	582 843.1	180.11	36.89	36.7	0.19
		2	583 100.70	582 920.3	180.40	114.38	113.9	0.29
2s3d	^3D	1	600 964.57	600 748.9	215.67			
		2	600 974.73	600 758.9	215.83	10.16	10.0	0.16
		3	600 994.61	600 779.2	215.41	30.04	30.3	−0.42
	^1D	2	612 856.04	612 615.6	240.44			

show in the next section can be used in the estimation of accuracy. All other reported data are based on BP line strengths in the length form. For each atom or ion, an ASCII file may be viewed or downloaded that contains all the information about the transitions in floating point form, suitable for processing.

6. Accuracy of Breit–Pauli energies

The accuracy of computed oscillator strengths and transition rates depends not only on the line strength but also on the transition energies. The latter can often be measured more accurately than computed, and computed transition data can be improved through scaling so that, in effect, the observed transition energy is used. However, for the production of large amounts of data this is not practical since, particularly for more highly ionized systems, the data may not be available. Our aim in this paper is to predict transitions to within a fraction of a per cent. This, of course, is more easily achieved when the transition energy is large than when it is small.

Table 4 compares the computed spectrum with observation for O v, where both correlation and relativistic effects are important. The difference in the excitation energies (theory–observed) appears to be largest for the $2p^2$ configuration, possibly because of the neglect of core correlation. In all other cases, the difference is a few 100 cm^{-1}. The splitting is reported too. It is defined here to be the energy with respect to the lowest level of the multiplet so that this value for the highest level gives the spread of the multiplet. The latter is a useful measure of the adequacy of the BP approximation, as will be described in the next section. All the theoretical energies and splittings were computed from variational total energies with somewhat more precision than displayed in this table.

As an example of some of the data available at the internet site, table 5 shows a portion of the E1 line list and associated data. Omitted are some of the intercombination lines with small transition rates. This is fully *ab initio* data.

Table 5. A portion of the computed line list data for O v. Omitted are some of the intercombination lines with small transition rates. The notation E + n denotes $\times 10^n$.

Multiplet	J_i–J_k	E (cm^{-1})	S	gf	A_{ki} (s^{-1})
2s3p ^{3}P$^o_0$–2s3d ^{3}D	2–1	17 863.87	0.105 9	0.005 75	4.076 74E+05
	2–2	17 874.03	1.589 2	0.086 28	3.677 42E+06
	2–3	17 893.91	8.907 1	0.484 13	1.477 13E+07
	1–1	17 941.36	1.587 9	0.086 54	6.193 51E+06
	1–2	17 951.52	4.766 0	0.259 88	1.117 25E+07
	0–1	17 978.25	2.119 1	0.115 73	8.316 68E+06
2s3s ^{1}S–2s3p ^{1}P^o	0–1	19 527.56	3.621 7	0.214 83	1.821 40E+07
2s3p ^{1}P–2s3d ^{1}D	1–2	31 828.15	6.898 0	0.666 89	9.012 63E+07
2s3s ^{3}S–2s3p ^{3}P^o	1–0	35 832.62	1.479 1	0.160 99	1.378 80E+08
	1–1	35 869.51	4.434 7	0.483 18	1.382 23E+08
	1–2	35 947.00	7.398 8	0.807 89	1.392 67E+08
2s2p ^{1}P^o–2p^2 ^{1}D	1–2	73 186.79	2.118 5	0.470 96	3.365 28E+08
2s^2 ^{1}S–2s2p ^{3}P^o	0–1	82 122.69	0.000 0	0.000 00	2.287 54E+03
2s2p ^{1}P^o–2p^2 ^{1}S	1–0	129 501.18	0.870 8	0.342 54	3.831 83E+09
2s2p ^{3}P^o–2p^2 ^{3}P	2–1	131 521.39	0.596 6	0.238 35	9.167 09E+08
	1–0	131 671.75	0.477 3	0.190 89	2.207 52E+09
	2–2	131 790.35	1.790 0	0.716 56	1.660 32E+09
	1–1	131 828.68	0.358 0	0.143 35	5.539 18E+08
	0–1	131 965.82	0.477 3	0.191 34	7.408 97E+08
	1–2	132 097.63	0.596 8	0.239 46	5.574 27E+08
2s^2 ^{1}S–2s2p ^{1}P^o	0–1	158 933.17	1.059 8	0.511 63	2.873 47E+09
2p^2 ^{1}S–2s3p ^{1}P^o	0–1	292 593.54	0.005 7	0.005 05	9.620 03E+07
2p^2 ^{1}D–2s3p ^{1}P^o	2–1	348 907.93	0.072 8	0.077 21	2.089 78E+09
2p^2 ^{1}D–2s3p ^{3}P^o	2–1	350 903.25	0.000 1	0.000 07	1.827 03E+06
	2–2	350 980.74	0.000 0	0.000 00	3.307 98E+03
2p^2 ^{3}P–2s3p ^{3}P^o	2–1	368 802.90	0.000 7	0.000 79	2.397 61E+07
	2–2	368 880.39	0.002 2	0.002 46	4.464 97E+07
	1–0	369 034.96	0.000 6	0.000 64	5.791 40E+07
	1–1	369 071.85	0.000 4	0.000 48	1.462 17E+07
	1–2	369 149.34	0.000 7	0.000 83	1.502 01E+07
	0–1	369 228.78	0.000 6	0.000 65	1.962 36E+07
2s2p ^{1}P^o–2s3s ^{1}S	1–0	402 567.17	0.043 2	0.052 77	5.704 30E+09
2s2p ^{1}P^o–2s3d ^{1}D	1–2	453 922.87	1.131 7	1.560 46	4.289 32E+10
2s2p ^{3}P^o–2s3s ^{3}S	2–1	464 723.74	0.151 0	0.213 21	1.023 82E+10
	1–1	465 031.02	0.090 4	0.127 63	6.136 79E+09
	0–1	465 168.16	0.030 1	0.042 50	2.044 49E+09
2s2p ^{3}P^o–2s3d ^{3}D	2–1	518 534.60	0.020 3	0.032 01	1.913 76E+09
	2–2	518 544.77	0.304 8	0.480 10	1.722 17E+10
	2–3	518 564.64	1.706 1	2.687 43	6.886 31E+10
	1–1	518 841.88	0.304 6	0.479 99	2.872 90E+10
	1–2	518 852.05	0.913 4	1.439 60	5.170 15E+10
	0–1	518 979.02	0.405 9	0.639 87	3.831 87E+10
2s^2 ^{1}S–2s3p ^{1}P^o	0–1	581 027.90	0.226 3	0.399 55	2.999 10E+10
2s^2 ^{1}S–2s3p ^{3}P^o	0–1	583 132.64	0.000 1	0.000 26	1.988 90E+07

The errors (in %) for all the excitation energies are reported in table 6. All are well below the 1% level. This, however, does not guarantee a similar accuracy for all transition energies. In table 7 are reported, first the difference in the length and velocity form of the line strength (in % with respect to the average $(S_l + S_v)/2$) of the LS calculation and then the error (in %) in the transition energy from the BP calculation.

Table 6. Excitation energy differences (in %) from NIST tabulated data [33] unless indicated otherwise.

		Z								
Term	*J*	4	5[a]	6	7	8	9[a]	10[a]	11	12
2s2p ^{3}P^o	0	0.54	0.08	0.05	0.04	0.05	0.12	0.17	0.29	0.46
	1	0.54	0.09	0.05	0.04	0.05	0.12	0.17	0.29	0.46
	2	0.54	0.09	0.05	0.04	0.05	0.12	0.17	0.29	0.46
2s2p ^{1}P^o	1	0.34	0.11	0.09	0.08	0.08	0.10	0.14	0.20	0.30
2p^2 ^{3}P	0	0.16	0.22	0.17	0.15	0.15	0.19	0.24	0.35	0.51
	1	0.16	0.22	0.17	0.15	0.16	0.19	0.24	0.35	0.51
	2	0.16	0.22	0.17	0.15	0.16	0.19	0.24	0.35	0.51
2p^2 ^{1}D	2	0.11	0.23	0.18	0.17	0.17	0.20	0.24	0.36	0.51
2p^2 ^{1}S	0		0.18	0.20	0.18	0.18	0.19	0.24	0.31	0.43
2s3s ^{3}S	1	0.00	0.02	0.03	0.03	0.03	0.04	0.04	0.07	0.09
2s3s ^{1}S	0	0.19	0.10	0.04	0.04	0.04	0.05	0.04	0.06	0.09
2s3p ^{1}P^o	1	0.08	0.04	0.04	0.04	0.04	0.04	0.04	0.05	0.07
2s3p ^{3}P^o	0	0.11	0.04	0.03	0.03	0.03	0.03	0.04		
	1	0.11	0.04	0.03	0.03	0.03	0.04	0.04		
	2	0.11	0.05	0.03	0.03	0.03	0.04	0.04		
2s3d ^{3}D	1	0.18	0.06	0.05	0.04	0.04	0.04	0.04	0.05	0.06
	2	0.18	0.06	0.05	0.04	0.04	0.04	0.04	0.05	0.06
	3	0.18	0.06	0.05	0.04	0.04	0.04	0.04	0.05	0.06
2s3d ^{1}D	2	0.09	0.06	0.05	0.04	0.04	0.04	0.04	0.05	0.06

[a] From Kelly [17].

7. Recommended values and estimates of accuracy

Theoretical transition rates can be improved by scaling to the observed transition energy. Let t (for transition) be defined as

$$t = \Delta E_{\rm obs}/\Delta E_{\rm th}. \tag{6}$$

Then, for allowed transitions, the recommended *normalized* gf value is

$$gf(\text{norm}) = t \times gf_l(\text{th}) \tag{7}$$

where gf_l(th) is the computed length value that correctly includes relativistic effects of lowest order. In this work, the relativistic effects on allowed transitions are not large. If we assume that the error is due primarily to the neglected correlation, then we propose an uncertainty estimate that is based, in part, on the difference in the two forms of the LS line strength. But agreement in length and velocity is a necessary, though not sufficient, condition for accuracy: the transition energy also needs to be correct. Let c be the relative discrepancy in the length and velocity forms of the LS average line strength, and e be the relative error in the LSJ transition energy: namely,

$$c = 2|S_l - S_v|/(S_l + S_v) \qquad \text{and} \qquad e = |\Delta E_{\rm th} - \Delta E_{\rm obs}|/\Delta E_{\rm obs}. \tag{8}$$

Then we propose an uncertainty estimate of $(c + e)gf$(norm). In some earlier work [18] on allowed transitions, using non-relativistic line strength but scaling for the transition energy, the formula $(1.5c + 0.1e)gf$(norm) was proposed. We will evaluate these hypotheses in the next section.

For intercombination lines, where gf values are extremely small, transition rates are usually reported rather than oscillator strengths. These depend on the mixing of terms, which,

Table 7. Accuracy indicators for allowed transitions. The first line shows the differences between S_v and S_l (in %) and the second line the differences (in %) between computed BP transition energies and transition energies from NIST data (average for each term).

	Z								
Transition	4	5	6	7	8	9	10	11	12
$2s^2\,{}^1S$–$2s2p\,{}^1P^o$	0.18	−0.09	−0.11	−0.12	−0.12	−0.11	−0.11	−0.10	−0.10
	0.34	0.08	0.05	0.04	0.04	0.04	0.05	0.06	0.09
$2s^2\,{}^1S$–$2s3p\,{}^1P^o$	0.15	0.09	0.02	0.02	0.03	0.03	0.03	0.03	0.03
	0.08	0.13	0.04	0.04	0.04	0.04	0.04	0.05	0.07
$2s2p\,{}^3P^o$–$2s3d\,{}^3D$	2.76	0.24	0.12	0.08	0.05	0.04	0.04	0.03	−0.03
	−0.02	0.05	0.05	0.04	0.03	0.03	0.02	0.03	0.02
$2s2p\,{}^3P^o$–$2p^2\,{}^3P$	−0.09	0.32	0.31	0.30	0.28	0.26	0.21	0.22	0.21
	−0.06	0.31	0.26	0.23	0.22	0.24	0.28	0.39	0.55
$2s2p\,{}^3P^o$–$2s3s\,{}^3S$	2.61	0.72	0.50	0.35	0.31	0.25	0.22	0.20	0.17
	−0.40	−0.002	0.02	0.09	0.03	0.03	0.03	0.04	0.05
$2s2p\,{}^1P^o$–$2p^2\,{}^1D$	−128	1.02	0.95	0.86	0.78	0.71	0.65	0.60	0.56
	−0.57	0.53	0.42	0.37	0.37	0.40	0.46	0.67	0.93
$2s2p\,{}^1P^o$–$2s3d\,{}^1D$	−4.55	−0.28	−0.17	−0.13	−0.10	−0.08	−0.07	−0.06	−0.05
	−0.40	0.01	0.03	0.02	0.02	0.02	0.01	0.02	0.01
$2s2p\,{}^1P^o$–$2p^2\,{}^1S$	—	0.05	0.16	0.19	0.19	0.19	0.18	0.17	0.16
	—	0.27	0.33	0 .31	0.30	0.31	0.36	0.45	0.58
$2s2p\,{}^1P$–$2s3s\,{}^1S$	−3.77	17.46	−0.95	−0.85	−0.70	−0.60	−0.52	−0.47	−0.44
	0.31	3.25	0.01	0.01	0.02	0.03	0.02	0.03	0.04
$2p^2\,{}^3P$–$2s3p\,{}^3P^o$	−199	10.93	0.17	−0.53	−0.44	−0.27	−0.22	−0.19	−0.17
	3.57	−0.35	−0.13	−0.06	−0.04	−0.04	−0.05	—	—
$2p^2\,{}^1D$–$2s3p\,{}^1P^o$	−6.00	−1.89	−2.26	−2.26	−1.78	−1.61	−1.45	−1.34	−1.25
	−0.55	−0.43	−0.16	−0.08	−0.06	−0.05	−0.06	−0.07	−0.08
$2s3s\,{}^3S$–$2s3p\,{}^3P^o$	1.78	0.42	0.29	−0.19	0.12	0.11	0.16	0.15	0.11
	1.01	0.26	0.08	0.05	−0.01	−0.11	−0.13	—	—
$2p^2\,{}^1S$–$2s3p\,{}^1P^o$	—	0.39	−0.28	0.02	0.06	0.04	−0.05	0.04	0.05
	—	−1.06	−0.33	−0.17	−0.11	−0.09	−0.09	−0.09	−0.10
$2s3s\,{}^1S$–$2s3p\,{}^1P^o$	−2.25	−0.69	−0.30	−0.37	−0.43	−0.32	−0.24	−0.19	−0.19
	−1.13	−0.78	−0.01	0.07	−0.06	−0.20	−0.28	−0.42	−0.67
$2s3p\,{}^1P^o$–$2s3d\,{}^1D$	−0.23	0.40	0.36	0.43	0.21	0.21	0.19	0.19	0.18
	0.28	0.33	0.22	0.15	0.09	0.07	0.05	0.03	−0.26
$2s3p\,{}^3P^o$–$2s3d\,{}^3D$	5.90	−0.22	−0.43	−0.35	−0.29	−0.27	−0.24	−0.23	−0.22
	1.38	0.30	0.38	0.28	0.19	0.13	0.08	—	—

in turn, depend on the separation of these terms. As first shown by Fleming *et al* [19], by using the observed term energy separation, the theoretical transition rates can be improved. Usually, only one term is an important player. For example, in the $2s^2\,{}^1S_0$–$2snp\,{}^3P^o_1$ transitions, the important mixing is between the terms of $2snp$ and, to first order, the mixing is proportional to the square of the inverse of the term separation. Let s (for separation) be defined as

$$s = \Delta E_{\mathrm{obs}}({}^1P^o_1\text{–}{}^3P^o_1)/\Delta E_{\mathrm{th}}({}^1P^o_1\text{–}{}^3P^o_1) \tag{9}$$

then a normalized transition rate is

$$A(\mathrm{norm}) = t^3 A(\mathrm{th})/s^2. \tag{10}$$

The uncertainty is now based on two factors, the uncertainty in the line strength of the primary 'allowed' transition and the uncertainty in the relativistic (BP) mixing of terms. It was further suggested by Fleming *et al* [19] and Hibbert [20] that the latter was related to the spread in the

fine-structure. Let r (for relativistic) be defined as

$$r = \Delta E_{\mathrm{obs}}(^3\mathrm{P}^{\mathrm{o}}_2\text{–}^3\mathrm{P}^{\mathrm{o}}_0)/\Delta E_{\mathrm{th}}(^3\mathrm{P}^{\mathrm{o}}_2\text{–}^3\mathrm{P}^{\mathrm{o}}_0). \tag{11}$$

Then a 'fine-tuned' value is

$$A(\mathrm{fine}) = r^2 A(\mathrm{norm}). \tag{12}$$

When core correlation is omitted, as in this paper for all but Be I, it has been shown [7] that A(fine) is in good agreement with experiment and is our recommended value. For converged results, we propose the uncertainty in A, say ΔA, as

$$\Delta A = |A(\mathrm{fine}) - A(\mathrm{norm})| + (|c| + |e|)A(\mathrm{norm}). \tag{13}$$

This scheme is similar to the one recommended by Brage *et al* [21] for the estimation of errors in Be-like intercombination lines where, in effect, the error in the transition energy, e, was ignored.

For the forbidden transitions, Fleming *et al* [22] propose a similar scheme. To obtain recommended values, we first scale to the observed transition energy. In general, transition rates scale as

$$A(\mathrm{scaled}) = t^{2\lambda+1} A(\mathrm{th}) \tag{14}$$

where $\lambda = 1$ for E1 and M1 transitions and $\lambda = 2$ for E2 and M2 transitions. Then, if the transition depends on mixing, similar factors need to be considered as in the case of intercombination lines. In the present case, such mixing is negligible and the only adjustments are scaling to the observed transition energy. In the next section we apply some of these ideas when comparing present work with other theories, experiment, or semi-empirical experimental predictions obtained from smoothing of experimental data.

8. Comparison with previous results, experiment, and semi-empirical evaluations

Some of the transitions included in this work have been benchmark calculations for the MCHF + BP method. In all of these, core correlation was included and present results will not be quite as accurate. Many comparisons can be found in earlier publications without particular concern about relativistic effects. A method much like MCHF + BP that also diagonalizes a BP Hamiltonian is CIV3 [19, 20] except that orbitals are analytic and are optimized in a carefully selected manner as determined by the problem. When relativistic effects are expected to be small, non-relativistic MCHF calculations, denoted MCHF(nr), may be used for the line strength along with observed transition energies in the oscillator strength calculation [18]. For Be, full core plus correlation (FCPC) results are similar in that relativistic effects are not included in the calculation of the line strength [28]. Fully relativistic methods include the MCDF method and relativistic many-body perturbation (RMBPT) methods that also include the Breit correction. Although the Breit correction in MCDF calculations based on the Dirac–Coulomb Hamiltonian is not as important in allowed transitions, they are extremely important in intercombination lines [23].

In table 8, the gf values of the $2s^2\,{}^1\mathrm{S}_0$–$2s2p\,{}^1\mathrm{P}^{\mathrm{o}}_1$ and $2s^2\,{}^1\mathrm{S}_0$–$2s3p\,{}^1\mathrm{P}^{\mathrm{o}}_1$ transitions are compared with benchmark calculations, recent results from either theory or experiment, and, at least for the former transition, two collections of experimental data that have been iso-electronically smoothed. There is variation in the latter. The Reistad and Martinson iso-electronically smoothed values [30] used fewer experimental values than those reported in [25] which included some higher Z values. The newly reported gf values for Be I and B II [24] are significantly larger than the ones used by Reistad and Martinson [30] and would change their smoothed values a lot. Possibly with this new data, their error bars could be reduced. It

should be mentioned that the validity of the smoothing procedure was already been raised by Fleming *et al* [32]. Also included in the table are semi-empirical (SE) values that analyse the allowed and intercombination transitions simultaneously, deriving a mixing angle for singlet–triplet mixing. This theory has been applied to both allowed transitions. Relativistic effects play a minor role in the allowed transitions and so semi-empirical values for the former transition are generally close to the iso-electronically smoothed experimental values. For the $2s^2\,{}^1S_0$–$2s3p\,{}^1P^o_1$ transitions, the line strength is considerably smaller and the singlet–triplet mixing less readily determined since, in fact, in B II the two states are almost degenerate, with ${}^3P^o$ slightly lower, and thereafter the ${}^1P^o$ being the lower state. Thus a smooth mixing angle is not likely to be valid. Since 2s3p is an excited configuration, branching ratios are needed before transition rates can be extracted from measured lifetimes. All these difficulties are reflected in the much larger differences between the SE and present work values for the latter transition.

Experimental data for $2s^2\,{}^1S_0$–$2s2p\,{}^1P^o_1$ is available for all these spectra except F VI. Here we report the NIST tabulations for the oscillator strengths which references indicate were obtained from theory dating back to 1964 and was given an accuracy rating of 'E' for uncertainties larger than 50%. For $2s^2\,{}^1S_0$–$2s3p\,{}^1P^o_1$ far more experimental oscillator strengths are missing. However, since it is important to be able to compare with the experimental transition energy as tabulated by NIST, we also include the NIST gf values along with accuracy classifications.

Not unexpectedly, this paper agrees best with other theories, especially when theories are normalized to the observed transition energy, a scaling often omitted by theorists. It is interesting to note the uncertainty estimates which in this case are based entirely on the discrepancy in length and velocity forms of the LS line strength and the error in the transition energy. For the $2s^2\,{}^1S_0$–$2s2p\,{}^1P^o_1$ transitions the uncertainty estimates appear reasonable. In fact, the normalized values are in near-perfect agreement to four significant digits with *all* normalized MCDF values [6, 23, 25] which is remarkable. The good agreement with the MCHF(nr) results of Jönsson *et al* [18] is an indication that relativistic effects on the line strength in the length form are not large. It is noted that the uncertainty estimates of their results and present work are similar. On the other hand, the errors in their energies are much larger but the formula used for determining uncertainties included only 10% of the error in the energy, whereas in this paper we have included 100% of this error in computing uncertainties. At the same time, the two results are within their uncertainties. Not included are the Safronova *et al* [39] RMBPT results which use only a first-order theory for obtaining coupling coefficients. For Mg IX, which could be expected to be the most accurate in our range of Z, their quoted A-rate would convert to a gf-value of 0.292, quite a bit smaller than the experimental and theoretical values included in table 8.

Although comparison with other theories like MCDF for $2s^2\,{}^1S_0$–$2s2p\,{}^1P^o_1$ suggests that maybe the formula for uncertainties produces uncertainties that are too large, they seem unreasonably small for $2s^2\,{}^1S_0$–$2s3p\,{}^1P^o_1$. The present values have not included core correlation effects, effects included in the earlier MCHF study, where systematic effects and extrapolation were included in deriving the uncertainty estimates. The RMBPT results of Safronova *et al* [38], were expected to be in error by several per cent in this energy range, improving as Z increases. Although matrix elements were computed to second order, the coupling coefficients (in jj) were computed only to first order. This is not expected to introduce large errors for the allowed transition, but they are large enough that no clear decision can be made with regard to the accuracy of our uncertainty estimates.

In table 9, the transition rates for the $2s^2\,{}^1S_0$–$2s2p\,{}^3P^o_1$ and $2s^2\,{}^1S_0$–$2s3p\,{}^3P^o_1$ intercombination lines are compared with benchmark calculations. All MCHF results are fine-

Table 8. Comparison of adjusted oscillator strengths for the allowed $2s^2\,{}^1S_0$–$2s2p\,{}^1P^o_1$ and $2s^2\,{}^1S_0$–$2s3p\,{}^1P^o_1$ transitions. The present oscillator strengths have been converted to observed transition energies with uncertainties determined from the discrepancy in the length and velocity forms of the line strength (see the text). Oscillator strengths from NIST tabulations are followed by their accuracy rating.

	$2s2p\,{}^1P^o_1$				$2s3p\,{}^1P^o_1$			
Element	ΔE (cm^{-1})	gf	Source	Ref.	ΔE (cm^{-1})	gf	Source	Ref.
Be I	42 565	1.40(6)	Experiment[a]	[24]	60 187	—	NIST	[33]
		1.339	Experiment[a]	[25]				
		1.341 7	SE	[26]				
	42 591	1.375(7)	MCHF+CIV3	[27]				
	42 749	1.371 1	MCHF(nr)	[18]	60 189	0.008 85(5)	MCHF	[35]
	42 569	1.374	FCPC	[28]	60 194	0.009 14(1)	FCPC	[28]
	42 604	1.375	Mod. Pot.	[29]	60 226	0.009 01	Mod. Pot.	[29]
	42 693	1.372 6(21)	Present work		60 233	0.009 0(2)	Present work	
B II	73 397	0.98(6)	Experiment[a]	[24]	144 103	—	NIST	[33]
		0.981	Experiment[a]	[25]				
		0.970 1	SE	[26]		0.075 8	SE	[36]
	73 655	0.997 6(22)	MCHF(nr)	[18]				
	73 592	0.998 5	MCDF[b]	[23]				
	73 530	0.994 8(23)	MCHF	[23]	144 099	0.109 3(3)	MCHF	[35]
	73 483	0.998 6(16)	Present work		144 177	0.108 4(2)	Present work	
C III	102 352	0.754(14)	Experiment[a]	[30]	258 931	0.232(B)	NIST	[37]
		0.760	Experiment[a]	[25]				
		0.754 1	SE	[26]		0.197 9	SE	[36]
	102 440	0.757 9(4)	MCDF[b]	[6]	259 309	0.267	RMBPT	[38]
	102 598	0.756 7(20)	MCHF(nr)	[18]				
	102 403	0.756	MCHF	[3]	258 922	0.241 4(4)	MCHF	[35]
	102 447	0.757 5(12)	Present work		259 035	0.240 6(2)	Present work	
N IV	130 694	0.620(14)	Experiment[a]	[30]	404 522	0.327(B)	NIST	[37]
		0.618	Experiment[a]	[25]				
		0.616 3	SE	[26]		0.285 8	SE	[36]
	130 830	0.609 3(16)	MCHF(nr)	[18]				
	131 029	0.610 2	MCDF[b]	[25]	404 654	0.341	RMBPT	[38]
	130 780	0.609 0(20)	MCHF+CIV3	[31]	404 504	0.333 8(4)	MCHF	[35]
	130 801	0.610 0(12)	Present work		404 666	0.333 1(2)	Present work	
O V	158 798	0.527(14)	Experiment[a]	[30]	580 525	0.392(B)	NIST	[37]
		0.520	Experiment[a]	[25]		0.353 3	SE	[36]
		0.521 2	SE	[26]	580 855	0.399	RMBPT	[38]
	158 709	0.510 5(14)	MCHF(nr)	[18]				
	159 154	0.511 1	MCDF[b]	[25]	580 791	0.400 3(5)	MCHF	[35]
	159 179	0.511	CIV3	[32]				
	158 933	0.511 2(10)	Present work		581 028	0.399 4(3)	Present work	
F VI	186 841	0.62(E)	NIST	[33]	787 844	0.478(E)	NIST	[33]
		0.451 7	SE	[26]		0.407 2	SE	[36]
	186 366	0.439 7(12)	MCHF(nr)	[18]	787 836	0.445	RMBPT	[38]
	187 224	0.440 5	MCDF[b]	[25]	787 777	0.450 0(5)	MCHF	[35]
	187 041	0.440 5(10)	Present work		788 140	0.448 7(3)	Present work	

Table 8. (Continued)

	$2s2p\,^1P^o_1$				$2s3p\,^1P^o_1$			
Element	ΔE (cm^{-1})	gf	Source	Ref.	ΔE (cm^{-1})	gf	Source	Ref.
Ne VII	214 952	0.395	Experiment[a]	[25]	1 025 650	0.448 9	SE	[36]
		0.398 8	SE	[26]	1 025 610	0.480	RMBPT	[38]
	213 894	0.386 7(11)	MCHF(nr)	[18]				
	215 350	0.387 5	MCDF[b]	[25]	1 025 488	0.488 4(6)	MCHF	[35]
	215 412	0.387	CIV3	[32]				
	215 260	0.387 5(10)	Present work		1 026 055	0.486 2(3)	Present work	
Na VIII	243 208	0.362(17)	Experiment	[34]	1 294 230	0.537(E)	NIST	[33]
		0.357 3	SE	[26]		0.483 3	SE	[36]
	243 625	0.346 4	MCDF[b]	[25]	1 294 180	0.508	RMBPT	[38]
	243 706	0.346 4(11)	Present work		1 294 895	0.514 7(4)	Present work	
Mg IX	271 687	0.319	Experiment[a]	[25]	1 593 600	0.508(B)	NIST	[33]
		0.323 9	SE	[26]		0.506 6	SE	[36]
	272 133	0.313 6	MCDF[b]	[25]	1 593 625	0.528	RMBPT	[38]
	272 178	0.313	CIV3	[32]				
	272 479	0.313 6(12)	Present work		1 594 738	0.535 1(5)	Present work	

[a] Smoothed experimental data.
[b] Scaled to observed transition energy.

tuned using observed data. For a core–valence calculation, both the fine-structure splitting and the A-rate are too large and fine-tuning tends to improve the final transition rate [7]. However, in B II, the observed fine-structure splitting has a rather large uncertainty and accurate studies which also include correlation in the core suggest a value of 22.19 [7] or 22.2 [44] cm^{-1}. In this case, our reported fine-tuned A-rate used the former theoretical splitting which yields a somewhat larger uncertainty.

For the $2s^2\,^1S_0$–$2s2p\,^3P^o_1$ transitions, the present work is in reasonable agreement with the semi-empirical model which should apply reasonably well. Like the present calculations, the MCDF values [25] for $Z \geqslant 7$ did not include core correlation yet are consistently somewhat smaller and outside our uncertainty limits. The latter appear reasonable in that there is overlap with somewhat more accurate results that include core correlation and also report uncertainties [21]. For the $2s^2\,^1S_0$–$2s3p\,^3P^o_1$ transition less data are available for comparision, but for all but B II there is good agreement with the SE transition rates, given the difficulty of the SE analysis for the decay from this excited state. Not included in this table are the recently published results of Safronova *et al* [38]. For the intercombination line, the coupling coefficients introduce extensive cancellation into the calculation and first-order coefficients are not sufficient for reliable data in this range of Z.

Finally, in table 10 we compare some of our transition energy adjusted data for forbidden transitions (first line of data) with those of Fleming *et al* [22, 31] based on a similar BP theory but including some core correlation (second line) and MCDF values [25, 45] (all other lines) where the former reference is to a core–valence calculation, whereas the latter also includes correlation with the core, but orbitals were constrained to be the same for both the initial and final state. Thus the values reported come from a variety of theories with different approximations. The BP with core correlation might be expected to be the most accurate, particularly at low Z, but the orbital set for [22] was an $n = 5 + 6p$ orbital set for core–valence correlation, a basis not particularly well suited for representing correlation in $1s^2$. The MCHF results of [31] include core correlation from the start and then proceed to an $n = 8$ orbital set optimizing on the primary $^3P^o$ term and determining an extra layer for the secondary $^1P^o$

Table 9. Comparison of present data (energies and adjusted transition rates) for some intercombination lines with other theory and experiment or the semi-empirical (SE) experimentally smoothed data. All energy data are from NIST tabulations [33]. The present transition rates are recommended values obtained from computed data along with uncertainties (see the text). The uncertainties for transition rates are given in parentheses (in units in the last place). The notation E + n denotes $\times 10^n$.

Element	$^3P^o_1$–$^1P^o_1$	$^3P^o_2$–$^3P^o_0$	ΔE (cm^{-1})	A_{ki} (s^{-1})	Source	Ref.
$2s^2\,^1S_0$–$2s2p\,^3P^o_1$						
B II	36 057	21.6±8	37 340	10.24(5)	Experiment	[40]
				9.15	SE	[36]
	36 225	22.19	37 303	10.27(20)	MCHF	[7]
	36 109	22.47	37 374	10.15(27)[a]	Present work	
C III	49 961	80.05	52 391	102.94(14)	Experiment	[8]
				102.35	SE	[36]
	50 112	79.72	52 357	103.0(4)	MCHF	[7]
	50 071	79.64	52 375	103.0(6)	MCHF	[21]
	50 070	80.05	52 370	102.9(1.5)	MCDF	[6]
	50 031	80.29	52 416	103.66(60)	Present work	
N IV	63 422	207.1	67 272	625(150)	Experiment	[41]
				583.7	SE	[36]
	63 728		67 301	557.8	MCDF[b]	[25]
	63 552	206.4	67 224	575.1(4)	MCHF	[21]
	63 502	207.6	67 298	578.4(27)	Present work	
O V	76 719	442.8	82 079	2.0(4)E+03	Experiment	[41]
				2332	SE	[36]
	77 050		82 104	2210	MCDF[b]	[25]
	76 719	442.8	82 001	2260(11)	MCHF	[21]
	77 144	440.4	82 035	2256.6	CIV3	[22]
	76 810	444.42	82 123	2276(16)	Present work	
Ne VII	103 242	1449.	111 705	2.2(11)E+04	Experiment	[42]
				19953	SE	[36]
	103 620		111 730	18608	MCDF[b]	[25]
	103 704	1442.5	11 708	19040.4	CIV3	[22]
	103 660	1452.41	111 896	19236(140)	Present work	
$2s^2\,^1S_0$–$2s3p\,^3P^o_1$						
B II	113	4.74	143 490	1.0E+05	SE	[36]
	126	4.68	144 189	2.7(6)E+05	MCHF	[43]
	127	4.67	144 053	2.9981(39)E+05	Present work	
C III	−780	18.75	259 711	4.0E+05	SE	[36]
	−769	18.82	259 818	5.0(2)E+05	MCHF	[43]
	−764	18.82	259 799	4.9705(62)E+05	Present work	
N IV	−1 465	51.2	405 988	2.8E+06	SE	[36]
	−1 451	51.59	406 131	3.2(1)E+06	MCHF	[43]
	−1 471	51.66	406 113	3.1937(36)E+06	Present work	
O V	−2 015	113.9	582 840	1.9E+07	SE	[36]
	−2 002	114.34	583 041	1.96(4)E+07	MCHF	[43]
	−1 995	114.38	583 023	1.9404(23)E+07	Present work	
F VI	−2 468	220.	790 316	1.0E+08	SE	[36]
	−2 457	221.06	790 610	9.89(9)E+07	MCHF	[43]
	−2 449	221.10	790 589	9.7608(130)E+07	Present work	

Table 9. (Continued)

Element	$^3P^o_1$–$^1P^o_1$	$^3P^o_2$–$^3P^o_0$	ΔE (cm^{-1})	A_{ki} (s^{-1})	Source	Ref.
Ne VII	−2 839	388.2	1 028 499	4.18E+08	SE	[36]
	−2 838	388.37	1 028 917	4.15(4)E+08	MCHF	[43]
	−2 829	388.51	1 028 884	4.1578(57)E+08	Present work	

[a] Fine-tuned using an accurate theoretical value of the term splitting [7].
[b] Scaled to observed transition energy.

Table 10. Comparison of present transition energy adjusted M1, E2, and M2 transition rates (in s^{-1}) from 2s2p $^3P^o$ with other theories. For each transition, the first line is present work, the second from other BP calculations, and the remaining from MCDF calculations, scaled to observed energies. The notation E + $(-)n$ denotes $\times 10^n$.

Z = 5		Z = 6		Z = 7		Z = 8		Z = 10		Z = 12	
A_{ki}	[Ref]	A_{ki}	[Ref]	A_{ki}	[Ref]	A_{ki}	[Ref]	A_{ki}	[Ref]	A_{ki}	[Ref]
$^3P^o_1$–$^3P^o_2$ M1											
5.795E−08		2.446E−06		4.070E−05		3.907E−04		1.333E−02		2.024E−01	
5.26E−08	[22]	2.33E−06	[22]	4.026E−05[a]	[31]	3.80E−04	[22]	1.30E−02	[22]	1.96E−01	[22]
		2.586E−06	[45]	4.118E−05	[45]	3.921E−04	[45]				
$^3P^o_0$–$^3P^o_1$ M1											
4.281E−09		2.378E−07		4.496E−06		4.631E−05		1.682E−03		2.568E−02	
3.80E−09	[22]	2.27E−07	[22]	4.516E−06[a]	[31]	4.62E−05	[22]	1.73E−03	[22]	2.77E−02	[22]
$^3P^o_0$–$^3P^o_2$ E2											
9.276E−16		1.482E−13		6.481E−12		1.335E−10		1.473E−08		5.437E−07	
7.93E−16	[22]	1.37E−13	[22]	6.415E−12[a]	[31]	1.23E−10	[22]	1.44E−08	[22]	5.41E−07	[22]
		1.344E−13	[45]	6.203E−12	[45]	1.308E−10	[45]				
$^3P^o_1$–$^3P^0_2$ E2											
4.152E−16		5.823E−14		2.389E−12		4.748E−11		5.072E−09		1.868E−07	
3.58E−16	[22]	5.37E−14	[22]			4.50E−11	[22]	4.81E−09	[22]	1.75E−07	[22]
		6.388E−14	[45]	2.435E−12	[45]	4.765E−11	[45]				
$^1S^o_0$–$^3P^o_2$ M2											
1.718E−03		5.203E−03		1.156E−02		2.167E−02		5.769E−02		1.253E−01	
1.72E−03	[22]	5.15E−03	[22]	1.144E−02	[31]	2.16E−02	[22]	5.77E−02	[22]	1.25E−01	[22]
1.698E−03[b]		5.139E−03	[6]	1.151E−02	[25]	2.154E−02	[25]	5.745E−02	[25]	1.247E−01	[25]
		5.130E−03	[45]	1.143E−02	[45]	2.151E−02	[45]				

[a] MCHF results.
[b] MCDF calculation including core correlation (unpublished).

term. These results, reported only for N IV, are expected to be the most accurate. For $Z = 7$, all the present transition rates agree to about 1% with these values. In B II, the present values for M1 and E2 transitions are 10–15% larger than the BP values of [22], but for higher Z agreement improves somewhat for M1 and E2 transitions. For the M2 transition, it was found that for the present core–valence model, the choice of 1s affected the rate more than in any other transition. The results reported here are based on separate calculations for 2s^2 $^1S_0$ where the 1s orbital was taken from simultaneous optimization of 2s2p $^{1,3}P^o$. A separate MCDF calculation was performed for the M2 transition in B II also including core correlation, normalized to the observed transition energy, which differs from the present work by 1%. Generally, all theories are in good agreement but the excellent agreement with the MCDF results based on independent optimization of the initial and final state [25] is reassuring: differences are at the 1% level.

9. Conclusions

In this paper we present an analysis of the transition data obtained for all transitions between levels of the Be-like energy spectrum where the most highly excited state is $2s3d\,^1D_2$, for $4 \leqslant Z \leqslant 12$. A simultaneous optimization scheme was used in the production of this data so that BP interactions could determine mixing of terms, removing some of the arbitrary decisions in other schemes such as the $(n, n+1)$ scheme where primary and secondary terms need to be designated: the choice is not obvious. In this work, it was assumed that the choice of 1s would not be critical, that a 1s obtained from an $n = 3$ valence correlation calculation for simultaneous optimization would provide the needed accuracy. Most transitions were not sensitive (at the 0.5% level) to this choice except for the M2 transition $2s^2\,^1S_0$–$2s2p\,^3P^o_2$. In retrospect, when the mixing from a different configuration is small, it would be more appropriate to determine the 1s from the state for which a basis is being determined as was done in the present work only for the ground state.

The present calculations did not include correlation in the core, except for Be I where there is less mixing of terms because of the much smaller relativistic effects. When a similar scheme is applied to the other first-row sequences, inclusion of core correlation will not be possible because of the larger size of the expansions that will be generated. Since the Be-like sequence has been studied so extensively, the present core–valence model could be validated as has been done here. An attempt has been made to find accuracy measures for transition energy adjusted data. Although length and velocity forms of the LS line strength can be expected to be critical factors, particularly when the transition energy has an error less than 1%, the errors in the adjusted oscillator strengths (or transition rates) may well be larger than the length and velocity discrepancy might indicate. For this reason, the error in the BP transition energy was also suggested as a factor. More accurate estimates require an analysis of trends (length and velocity may both be decreasing, for example) as well as other factors that depend on the computational model as was done for $2s^2\,^1S_0$–$2s3p\,^1P^o_1$ [35], for example.

The procedures described here lend themselves to the production of large amounts of data by fairly automatic schemes. The large BP calculations were performed on the T3E at the National Energy Research Scientific Computing Center (NERSC) using an MPI version of the code and employing 32 processors for large cases.

Acknowledgment

This research was supported by the Division of Chemical Sciences, Office of Basic Energy Sciences, Office of Science, US Department of Energy.

References

[1] Seaton M J 1996 *Phys. Scr.* T **65** 129
[2] The Opacity Team 1995 *The Opacity Project* (Bristol: Institute of Physics Publishing)
[3] Froese Fischer C 1994 *Phys. Scr.* **49** 51
[4] Godefroid M R, Froese Fischer C and Jönsson P 1996 *Phys. Scr.* T **65** 70
[5] Froese Fischer C 1999 *Phys. Scr.* T **83** 49
[6] Jönsson P and Froese Fischer C 1998 *Phys. Rev.* A **57** 4967
[7] Froese Fischer C and Gaigalas G 1997 *Phys. Scr.* **56** 436
[8] Doerfert J, Träbert E, Wolf A, Schwalm D and Uwira O 1996 *Phys. Rev. Lett.* **78** 4355
[9] Froese Fischer C, Saparov M, Gaigalas G and Godefroid M 1998 *At. Data Nucl. Data Tables* **70** 119
[10] Froese Fischer C, Brage T and Jönsson P 1997 *Computational Atomic Structure—An MCHF Approach* (Bristol: Institute of Physics Publishing)
[11] Davidson E R 1975 *J. Comput. Phys.* **17** 87

[12] Stathopoulos A and Froese Fischer C 1994 *Comput. Phys. Commun.* **64** 268
[13] Drake G W F 1972 *Phys. Rev.* A **5** 1979
[14] Olsen J, Godefroid M, Jönsson P, Malmqvist P Å and Froese Fischer C 1995 *Phys. Rev.* E **52** 4499
[15] Froese Fischer C and He X *Can. J. Phys.* at press
[16] Froese Fischer C 1984 *Phys. Rev.* A **30** 2741
[17] Kelly R L http://cfa-www.harvard.edu/amdata/ampdata /kelly/kelly.html
[18] Jönsson P, Froese Fischer C and Godefroid M R 1999 *J. Phys. B: At. Mol. Opt. Phys.* **32** 1233
[19] Fleming J, Hibbert A and Stafford R P 1994 *Phys. Scr.* **49** 316
[20] Hibbert A 1996 *Phys. Scr.* T **65** 104
[21] Brage T, Fleming J and Hutton R *Mon. Not. R. Astron. Soc.* in preparation
[22] Fleming J, Bell K L, Hibbert A, Vaeck N and Godefroid M R 1996 *Mon. Not. R. Astron. Soc.* **279** 1289–93
[23] Ynnerman A and Froese Fischer C 1995 *Z. Phys.* D **34** 1
[24] Irving R E, Henderson M, Curtis L J, Martinson I and Bengtsson P 1999 *Can. J. Phys.* **77** 137
[25] Jönsson P, Froese Fischer C and Träbert E 1998 *Phys. Rev.* A **31** 3497
[26] Curtis L J and Ellis D G 1996 *J. Phys. B: At. Mol. Opt. Phys.* **29** 645
[27] Fleming J, Godefroid M R, Bell K L, Hibbert A, Vaeck N, Olsen J, Jönsson P and Froese Fischer C 1996 *J. Phys. B: At. Mol. Opt. Phys.* **29** 4347–63
[28] Chung K T and Z-W Zhu 1993 *Phys. Rev.* A **48** 1944
[29] Chen M K 1998 *J. Phys. B: At. Mol. Opt. Phys.* **31** 4523
[30] Reistad N and Martinson I 1986 *Phys. Rev.* A **34** 2632
[31] Fleming J, Brage T, Bell K L, Vaeck N, Hibbert A, Godefroid M R and Froese Fischer C 1995 *Ap. J.* **455** 758
[32] Fleming J, Vaeck N, Hibbert A, Bell K L and Godefroid M R 1996 *Phys. Scr.* **53** 446–53
[33] Nist Database http://aeldata.nist.gov/nist_atomic_spectra.html
[34] Toirdoir X, Biémont E, Garnir H P, Dumont P-D and Träbert E 1999 *Eur. Phys. J.* D **6** 1
[35] Froese Fischer C, Godefroid M and Olsen J 1997 *J. Phys. B: At. Mol. Opt. Phys.* **30** 1163
[36] Curtis L J *et al* 1995 *Phys. Rev.* A **51** 4575
[37] Wiese W L, Fuhr J R and Deters T M 1996 Atomic Transition Probabilities of Carbon, Nitrogen, and Oxygen (*J. Phys. Chem. Ref. Data Monograph vol 7*) (Washington: American Chemical Society and Woodbury, NY: American Institute of Physics)
[38] Safronova U I, Dervianko A, Safronova M S and Johnson W R 1999 *J. Phys. B: At. Mol. Opt. Phys.* **32** 3527
[39] Safronova U I, Johnson W R, Safronova M S, and Dervianko A 1999 *Phys. Scr.* **59** 286
[40] Träbert E, Wolf A, Linemannn J and Tordoir X 1999 *J. Phys. B: At. Mol. Opt. Phys.* **32** 537
[41] Doerfert J, Träbert E, and Wolf A 1996 *Hyperfine Int.* **99** 155
[42] Kunze H-J 1972 *Space Sci. Rev.* **13** 565
[43] Froese Fischer C, Godefroid M and Gaigalas G 1997 *J. Phys. B: At. Mol. Opt. Phys.* **30** 3333
[44] Zhu X-W and Chung K T 1994 *Phys. Rev.* A **50** 3818
[45] Ynnerman A and Froese Fischer C 1995 unpublished. Based on wavefunctions obtained in *Phys. Rev.* A **51** 2020